Towards high-performance, low-cost quartz sensors with high-density, well-separated, vertically aligned ZnO nanowires by low-temperature, seed-less, single-step, double-sided growth

2013 Nanotechnology 24 355503

(http://iopscience.iop.org/0957-4484/24/35/355503)

Nanotechnology **24** (2013) 355503 (9pp) doi:10.1088/0957-4484/24/35/355503

Towards high-performance, low-cost quartz sensors with high-density, well-separated, vertically aligned ZnO nanowires by low-temperature, seed-less, single-step, double-sided growth

Andrea Orsini[1], Pier Gianni Medaglia[2], David Scarpellini[2], Roberto Pizzoferrato[2] and Christian Falconi[1]

[1] Department of Electronic Engineering, University of Tor Vergata, Via del Politecnico 1, I-00133, Rome, Italy
[2] Department of Industrial Engineering, University of Tor Vergata, Via del Politecnico 1, I-00133, Rome, Italy

E-mail: falconi@eln.uniroma2.it

Received 20 May 2013, in final form 16 July 2013
Published 7 August 2013
Online at stacks.iop.org/Nano/24/355503

Abstract
Resonant sensors with nanostructured surfaces have long been considered as an emergent platform for high-sensitivity transduction because of the potentially very large sensing areas. Nevertheless, until now only complex, time-consuming, expensive and sub-optimal fabrication procedures have been described; in fact, especially with reference to in-liquid applications, very few devices have been reported. Here, we first demonstrate that, by immersing standard, ultra-low-cost quartz resonators with un-polished silver electrodes in a conventional zinc nitrate/HMTA equimolar nutrient solution, the gentle contamination from the metallic package allows direct growth on the electrodes of arrays of high-density (up to 10 μm^{-2}) and well-separated (no fusion at the roots) ZnO nanowires without any seed layer or thermal annealing. The combination of high-density and good separation is ideal for increasing the sensing area; moreover, this uniquely simple, single-step process is suitable for conventional, ultra-low-cost and high-frequency quartzes, and results in devices that are already packaged and ready to use. As an additional advantage, the process parameters can be effectively optimized by measuring the quartz admittance before and after growth. As a preliminary test, we show that the sensitivity to the liquid properties of high-frequency (i.e. high sensitivity) quartzes can be further increased by nearly one order of magnitude and thus show the highest ever reported frequency shifts of an admittance resonance in response to immersion in both ethanol and water.

(Some figures may appear in colour only in the online journal)

Among all piezoelectric materials, quartz crystals are made from naturally abundant materials and uniquely offer many crucial advantages for the fabrication of electromechanical resonators, including easy and low-cost manufacture of high purity and almost-perfect crystals, extremely high quality factors, and the existence of cuts with zero temperature coefficient. Additionally, quartz oscillators can easily achieve high sensitivity, good long term stability, low power consumption, and low susceptibility to interference. For these reasons, quartz resonating sensors are widely used for

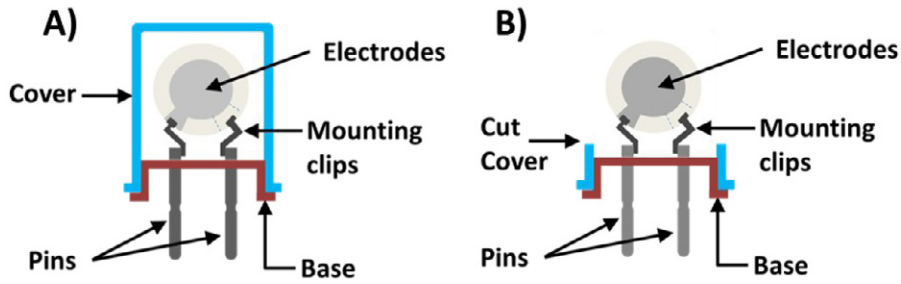

Figure 1. Sketch of a commercial, low-cost quartz resonator with an HC-49/U package (A) and the package opened by cutting the metallic cover (B).

the measurement of time, frequency, pressure, acceleration, temperature, forces, mass, liquid density/viscosity and concentrations of both chemical and biological quantities. In fact, several quartz resonators are commercially available, with a wide variety of products, including expensive voltage controlled, temperature compensated oscillators as well as very cheap resonators. As an example, figure 1(A) schematically shows a fully packaged resonator whose cost may be as low as a fraction of a dollar; as shown in figure 1(B), such packages can be easily opened by cutting the metallic cover near the base, thus making the electrodes accessible to chemicals.

In particular, quartz resonators which are used for measuring the mass deposited on the electrodes are often referred to as quartz crystal microbalances (QCMs) [1] and are widely used for sensing. Functionalization of the QCM electrodes with nanostructures obviously results in a substantially larger 'active' area, which may translate into higher sensitivity [2–7], especially in the case of quasi 1D nanostructures (e.g. nanowires, nanorods, nanoneedles, . . .). For instance, nanowires have been integrated onto the electrodes of a QCM (nano-QCM) by a three-step process consisting of the synthesis of the nanostructures (e.g. in a high-temperature furnace) followed by homogeneous dispersion of the nanostructures inside a solvent (e.g. ethanol) and by drop casting onto the QCM electrodes [8–12]; however, this technique has several disadvantages, including a limited increase of the exposed 'active' area, a degraded quality factor (due to the resulting random alignment of the nanowires which results in a position-dependent mechanical load), and a limited adhesion. Clearly, in order to obtain the highest possible active area, QCMs should be functionalized by growing dense arrays of vertically aligned and well-separated (i.e. with no fusion among the roots of distinct nanowires) nanostructures on the electrodes. Incidentally, such devices can also have other important applications; for instance, the high response of a ZnO nanostructure-based quartz crystal microbalance for biochemical sensing has been attributed to the super-hydrophilicity of the ZnO nanotips [13]; additionally, an electromechanical resonator with an array of vertically aligned nanostructures on the electrode may constitute a system of coupled resonators so that, if the resonant frequencies of the nanostructures and the resonator are well matched [14], a substantial increase of the sensitivity is possible.

However, despite the potential advantages of quartz resonators with arrays of vertically aligned nanowires on the electrodes, only few such devices have been reported so far, primarily due to technological issues. For instance, arrays of vertically aligned ZnO nanowires have been integrated onto QCM electrodes by using MOCVD (metal organic chemical vapour deposition) [15], but this technique is expensive, complex, requires high temperatures, and is difficult to implement for commercially available packaged resonators and for double-sided functionalization. Alternatively, arrays of ZnO nanowires have been grown on quartz resonators by wet chemistry [16] following the sputtering [17] or drop-coating [18, 19] deposition of a ZnO seed layer. However, the presence of a seed layer usually results in nanowires with fusion among their roots, thus reducing the exposed area; moreover, the seed layer can be deposited only on one side at a time; finally, the deposition of the seed layer in the case of thin and fragile high-frequency (i.e. high sensitivity) quartz resonators is problematic (in fact, no previously reported nano-QCMs employing a seed layer [17–19] have used quartzes with resonant frequencies higher than about 5 MHz), especially for low-cost commercially available quartzes, which are fixed by means of mounting clips to the base (e.g. see figure 1(A) for the HC-49/U package).

Nevertheless, to date there have been no reports of QCMs functionalized with high-density, vertically aligned nanostructures grown without a seed layer. In fact, although the conventional wet-chemistry synthesis of ZnO nanowires by means of an equimolar solution of zinc nitrate hexahydrate and hexamethylenetetramine (HMTA) has been used for the seed-less growth of *c*-axis oriented ZnO nanorods onto bare silver (111) [20] and gold (111) [21] surfaces, only low nanowire densities (about 1 μm^{-2}) and poor homogeneity could be obtained. High-density, homogeneous, and seed-less growth of ZnO nanowires onto metal surfaces has been obtained only by replacing HMTA with ammonium hydroxide in the nutrient solution, and with high concentrations of zinc nitrate [22, 23]; however, ammonium hydroxide is very corrosive and is not ideal for functionalizing commercial quartz resonators, because any corrosion and degradation of the electrical contacts could dramatically reduce the quality factor.

Here, as an extremely simple solution, we demonstrate that the gentle contamination from the package of low cost, commercially available quartz resonators in a conventional

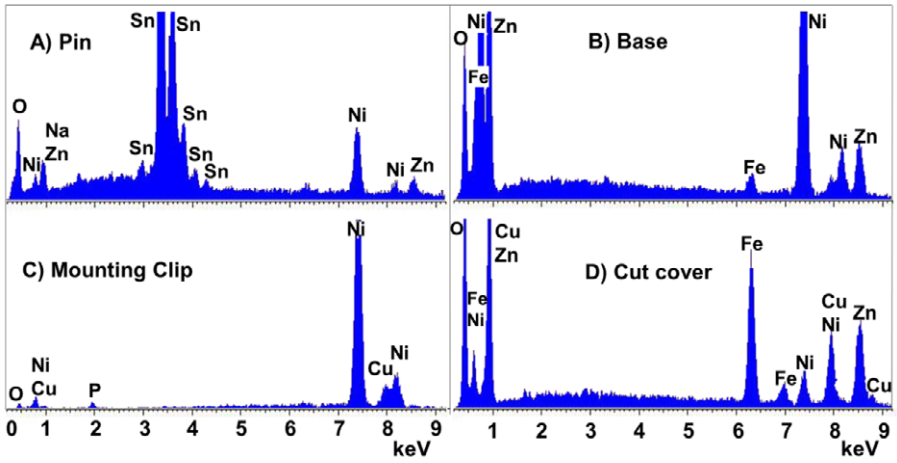

Figure 2. EDS patterns of the different parts of an HC-49/U package: (A) pin; (B) base; (C) mounting clip; (D) cut cover.

HMTA/zinc nitrate based solution allows the growth of vertically aligned ZnO nanowires on both of the silver electrodes of the quartz, with densities of up to 10 μm^{-2}, by means of a single, low-temperature, and easy fabrication step, without any seed layer, thermal annealing, or mechanical manipulation of the quartz. In particular, after opening the packages, we have successfully functionalized both the silver electrodes of AT-cut quartz resonators with resonant frequencies ranging from 3.5 to as high as 20 MHz. Our devices exhibited no detectable fusion among the roots of distinct nanowires and a single step was sufficient for functionalizing both the electrodes of the quartz. Energy-dispersive spectroscopy (EDS), x-ray diffraction (XRD) and photoluminescence (PL) demonstrate that the gentle contamination results in a very low doping and presence of defects in the nanowires. We also show that both the densities and the morphologies of the nanowires can be optimized by tuning the equimolar concentration of zinc nitrate and HMTA which, in our experiments, was changed between 0.5 and 5 mM. Furthermore, by measuring the impedance of the quartz resonator before and after the growth of nanowires, we accurately estimated the total deposited ZnO mass per unit area, which was maximum at a 2.5 mM equimolar concentration of zinc nitrate/HMTA. Finally, as a preliminary test, we have grown arrays of nanowires on both the electrodes of ultra-low-cost, high-frequency QCMs with silver electrodes, thus increasing the sensitivity to liquid properties by nearly one order of magnitude and obtaining the highest ever reported shifts of the QCM admittance resonance in response to immersion in both ethanol and water.

1. Results and discussion

Highly dense vertically aligned ZnO nanostructures were grown directly onto both the (111) un-polished silver electrodes of low-cost quartzes when the resonators were immersed, in the presence of their package (pins, base, cut cover, and mounting clips), into an equimolar solution of zinc nitrate hexahydrate and hexamethylenetetramine (HMTA) at low concentrations (from 0.5 to 5 mM) in order to provide zinc ions and a stabilized release of OH^- ions during the growth process at 90 °C [24]. Since the high-density nanowire growth could not take place on quartzes immersed without their package, in addition to the standard reactions for the growth of ZnO nanowires

$$C_6H_{12}N_4 + 6H_2O \rightarrow 6HCHO + 4NH_3 \quad (1)$$

$$NH_3 + H_2O \leftrightarrow NH_4^+ + OH^- \quad (2)$$

$$Zn^{2+} + 2OH^- \leftrightarrow ZnO + H_2O \quad (3)$$

we propose that the growth is promoted by the weak and slow package-induced contamination of the solution in the volume surrounding the quartz resonator. We have performed EDS analyses on different parts of several packages and found that their elemental composition is quite complex, including nickel, tin, iron, copper, and phosphorus; for instance, figure 2 shows the EDS spectra of the different parts of an HC-49/U package after the growth of ZnO nanowires.

Although the metallic package, when immersed in the solution for growing zinc oxide nanowires, may release several contaminants, iron species are most likely responsible for the substantially enhanced nucleation on the silver electrodes because Fe is very reactive and easily forms iron(III) hexahydrated complex ions, even in slightly acidic solutions. In fact, after the synthesis of nanowires, we have often found eye-detectable layers of oxidized iron species on parts of the package (especially on the cut cover). As another confirmation, SEM analysis revealed that ZnO nanostructures also grow on the package itself, especially on the cut cover, which is consistent with figure 2 (the maximum values of both the Zn and the Fe peaks are found on the cut cover, figure 2(D)). We stress that the proposed mechanism is also consistent with a study by Kokotov *et al*, who demonstrated that hydrated oxide colloids (FeOOH) can promote the high-density nucleation of ZnO nanowires on glass substrates [25].

Figure 3 shows typical SEM images of silver electrodes of QCMs after the growth of the ZnO nanorod vertical array with a zinc nitrate/HMTA equimolar concentration of 2.5 mM, a temperature of 90 °C, and a growth time

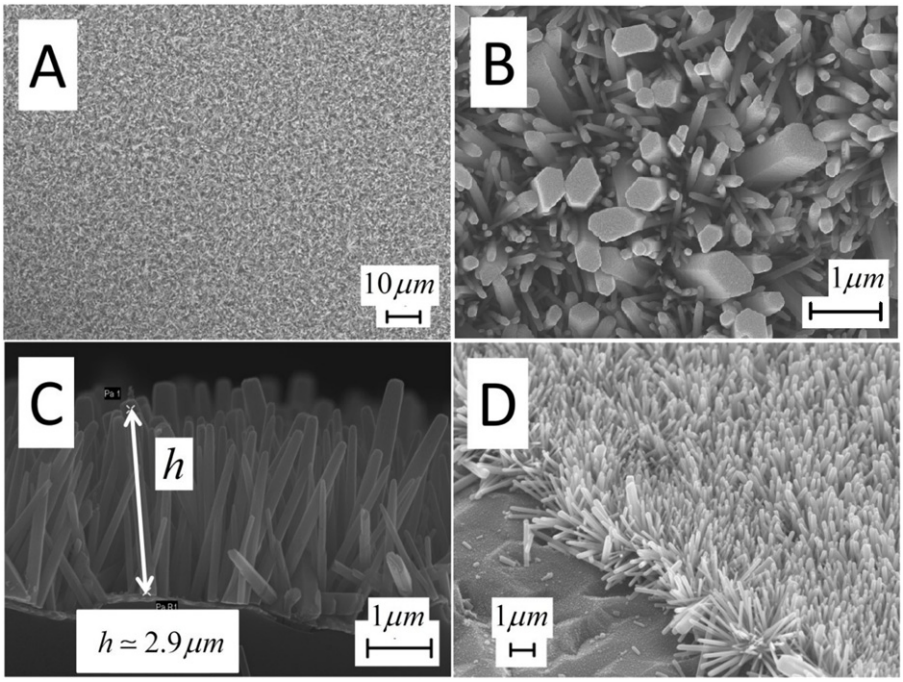

Figure 3. Typical SEM pictures of 20 MHz QCMs after synthesis of ZnO nanowires: (A) top view; (B) enlarged top view; (C) cross-section; (D) 45° tilted view of the border between the electrode and the quartz, showing that ZnO nanowires only grow on the silver electrode.

of about 12 h. As is evident from figure 3(B), the ZnO nanorods have a hexagonal shape with edges ranging from about 20 nm to more than 600 nm. The cross-section in figure 3(C) demonstrates that the height is relatively constant (about 3 μm) and the misalignment is mainly induced by the un-polished electrode surface. Moreover, as shown in figure 3(D), ZnO nanostructures only grow on top of the metal electrode and not on the quartz free surface, thus potentially providing a very convenient approach for co-integration of high-density ZnO nanowires into pre-existing CMOS/MEMS devices or flexible substrates, without any high-temperature step or any use of corrosive chemicals. The preferential nucleation of vertically aligned ZnO nanorods onto the silver surface is due to the very good in plane lattice match between the hexagonal wurtzite lattice of ZnO and the (111) plane of Ag that also has a hexagonal symmetry (only 11% narrower); on the other hand, there is practically no nucleation on the SiO_2 surface due to the large lattice mismatch between the AT-cut quartz lattice and ZnO [20, 21].

Figure 4 shows the top view of ZnO nanowires grown by using different equimolar concentrations of zinc nitrate and HMTA, with a temperature of 90 °C and a growth time of about 12 h. Figures 4(A) and (B) show that at low zinc nitrate/HMTA concentrations (0.5 and 1 mM) the nanostructures have a hexagonal base and a sharp tip. Figures 4(C) and (D) show that at higher concentrations (2.5 and 5 mM) ZnO nanorods with an almost constant cross-section along the *c*-axis are formed. The density of the ZnO nanorods at the higher concentrations of zinc nitrate (see figure 4(D)) is more than 10 nanorods per square micron, which is one order of magnitude greater than the value obtained for the growth of ZnO nanorods on silver or gold with a similar solution [20, 21] but without the gentle contamination from the metallic package.

In order to verify the effects of the metallic contamination on the nanowires, we performed energy-dispersive spectroscopy (EDS) and found only four elements, namely oxygen (ZnO nanowires and quartz), zinc (ZnO nanowires), silver (metal electrode) and silicon (quartz); therefore, we conclude that the package-induced contamination of the solution does not result in massive doping of the ZnO nanowires. As another confirmation, the *c*-axis lattice parameter of the ZnO nanorods, as taken from the (002) XRD peak position, is in agreement with the ZnO theoretical bulk value. Moreover, we also compared the room-temperature PL emission spectra of the nanorods grown onto the silver electrodes of the QCMs with the PL spectra of 'pure' ZnO nanorods grown, without any source of contamination, in an identical equimolar zinc nitrate/HMTA solution and collected on a gold-covered silicon substrate placed at the bottom of the container. Figure 5 reports the PL spectra of the two samples after normalization of the peaks of the low-energy bands for easier comparison. Both the spectra are similar to those reported in the literature for undoped and un-annealed ZnO nanostructures grown by a wet-chemistry method [26–28]. Specifically, the relatively narrow peak in the UV band at 3.26 eV (380 nm) is due to the near-band-edge (NBE) emission and the broad band peak in the visible range at approximately 2 eV is related to the deep-level emission (DLE) from intrinsic-defects and/or impurity states. Remarkably, with reference to figure 5, the ratio between the NBE and the DLE is close to unity and even slightly larger for the ZnO nanorods grown with the package contamination of the solution, indicating that the density of lattice defects is approximately the same as in

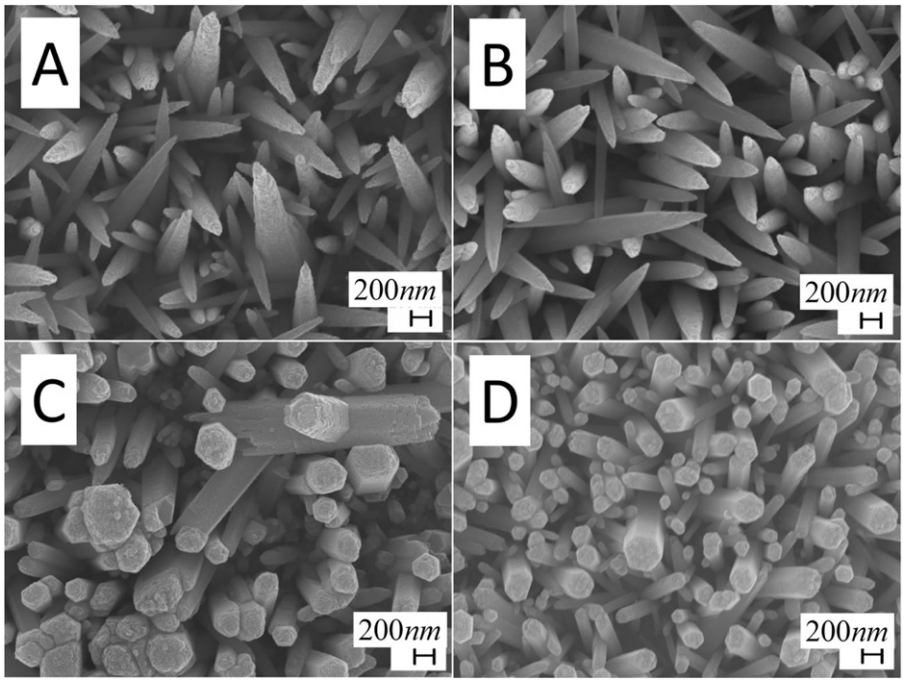

Figure 4. SEM pictures of the top view of 20 MHz QCM resonators after the ZnO growth of nanostructures at 90 °C and with different equimolar concentrations, C, of zinc nitrate and HMTA: (A) $C = 0.5$ mM; (B) $C = 1$ mM; (C) $C = 2.5$ mM; (D) $C = 5$ mM.

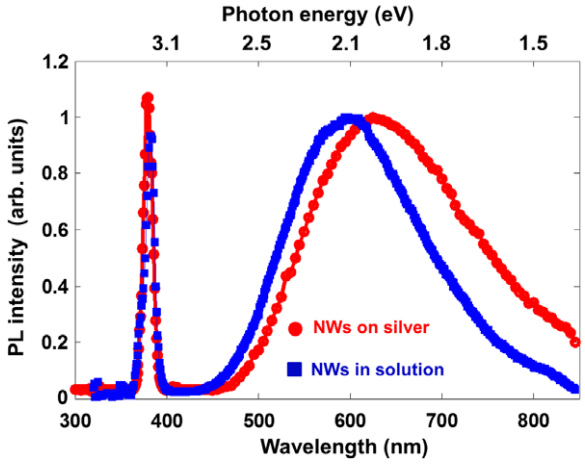

Figure 5. PL spectra of the ZnO nanowires epitaxially grown onto the silver electrode of a QCM (red line with circles) and grown in a solution in a separate container without any source of contamination (blue line with squares).

the nanowires grown in standard conditions (i.e. without any source of contamination). In summary, XRD, PL, and EDS measurements consistently confirm that the metallic contamination, although responsible for the high-density growth of nanowires, does not induce substantial additional defects in the ZnO lattice structure, so that the proposed method may also find other applications (e.g. nanogenerators and piezotronics).

The use of a quartz resonator as a substrate for growing nanostructure is also a fast and precise method for easily estimating the nanostructure's deposited mass and density. In fact, assuming that the ZnO nanorods behave as a rigid acoustic mass, the Sauerbrey equation relates the ZnO mass loading (Δm) on the electrode surface to the variation of the QCM resonant frequency (ΔF_R) as follows:

$$\Delta F_R = -2 \cdot f_0^2 \cdot C_q \cdot \Delta m, \tag{4}$$

where f_0 is the original resonant frequency of the QCM and C_q is a constant dependent on the physical properties of the quartz single crystal (its value for commercial AT-cut QCMs is 2269×10^{-15} Hz cm^2 ng^{-1} for a thin film coating on both the QCM electrodes). The Sauerbrey equation also illustrates that a higher initial resonant frequency, f_0, translates into higher sensitivities (i.e. higher variation of the resonant frequency for a given variation of the mass).

In our experiments we used a network analyser to separately record the real and the imaginary parts of the QCM admittance at frequencies around the resonant frequency F_R. Figure 6 shows the real part (always positive, blue curves) and the imaginary part (green curves) of the admittance of commercial QCMs before ((A), (C)) and after deposition ((B), (D)), for both a 3.58 MHz QCM ((A), (B)) and a 20 MHz QCM ((C), (D)).

The total mass of the deposited nanowires can be easily quantified by taking advantage of the frequency shift induced by the ZnO nanostructures on the QCM substrate. For instance, figure 7 illustrates the influence of the zinc nitrate/HMTA equimolar initial concentration, ranging from 0.5 to 5 mM, on the deposited ZnO nanowire mass by showing the final frequency shift (ΔF_R) for eight QCMs, with original resonant frequencies of 20 MHz (four QCMs, blue dots line) and 3.58 MHz (four QCMs, black squares line). The similar behaviour, obtained on different types of QCMs, confirms that the maximum increase of the resonant frequency shift (ΔF_R)

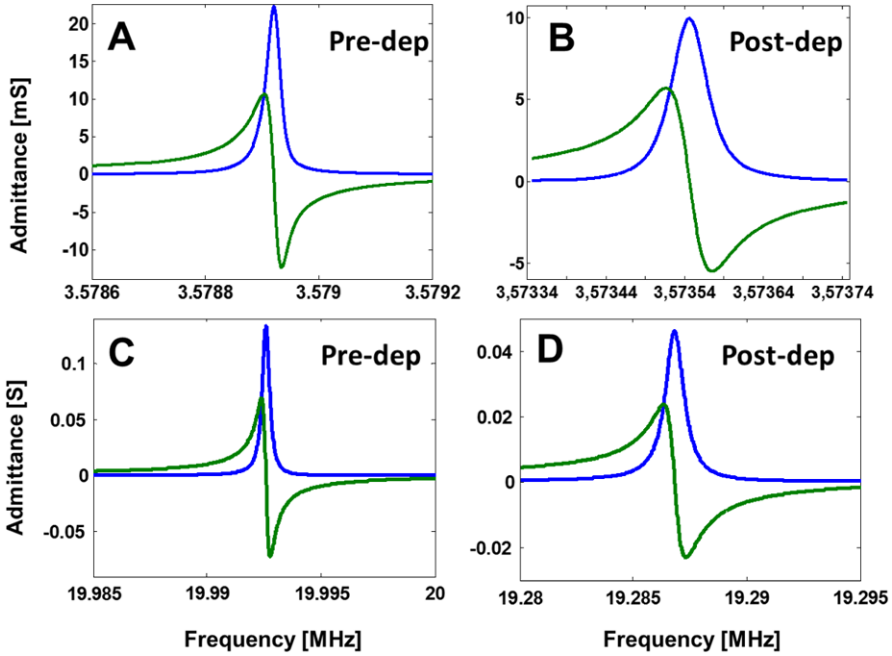

Figure 6. Real part (always positive, blue) and imaginary part (green) of the admittances of QCMs before and after the growth of ZnO nanowires. Admittance of a commercial quartz resonator with initial (nominal) resonant frequency equal to 3.58 MHz before (A) and after (B) the nanowire synthesis. Admittance of a commercial quartz resonator with initial (nominal) resonant frequency equal to 20 MHz before (C) and after (D) the nanowire synthesis.

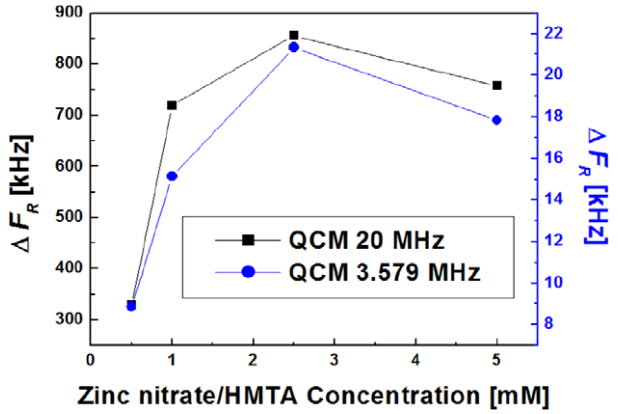

Figure 7. ΔF_R for eight QCMs used as substrates for the ZnO NW growth at four different equimolar concentrations of zinc nitrate/HMTA salts (0.5, 1, 2.5, and 5 mM), with a temperature of 90 °C and a growth time of about 12 h. Each data point corresponds to a different QCM with initial (nominal) resonant frequency of 20 MHz (black squares, four QCMs, *y*-axis on the left) or 3.58 MHz (blue circles, *y*-axis on the right).

is found at an equimolar concentration of 2.5 mM, which is much lower than previously reported values (20 mM [23] or 35 mM [22]), thus suggesting that the proposed growth method allows a much more effective use of the reagents. The frequency shifts for the 20 MHz QCMs are about 40 times higher than for the 3.58 MHz QCMs, which is in reasonable agreement with the Sauerbrey equation (which would predict a shift 31 times higher for the 20 MHz QCMs).

In order to show the potentialities of the proposed devices for high-performance sensing, as a preliminary test, we have repeatedly immersed in water and ethanol pairs of nominally identical, ultra-low-cost quartz resonators, with one quartz functionalized by ZnO nanorods (nano-QCM). First, we have used a pair of quartzes with initial (nominal) resonant frequencies equal to 20 MHz; the nano-QCM was obtained with salt concentration, growth temperature and time equal to 2.5 mM, 90 °C, and 12 h, respectively; although the responses to liquid immersion were very high, the quality factors of the resonators in liquids were very small. Therefore, in order to keep a satisfactory quality factor, we have used a pair of quartzes with initial (nominal) resonant frequencies equal to 16 MHz; the nano-QCM was obtained with salt concentration, growth temperature and time equal to 1 mM, 90 °C, and 4 h, respectively. Figure 8 shows the shifts of the resonant frequencies (ΔF_R) of the bare QCM (red line) and the 16 MHz nano-QCM (blue line) upon three consecutive immersions in DI water (figure 8(A)) and ethanol (figure 8(B)). The resonant frequency of the nano-QCM is much more sensitive to both in-liquid immersion and liquid properties, with frequency shifts which are about ten times larger. The higher response of the nano-QCM is due to the nano-textured surface, which strongly increases the mass loading and changes both the resonant frequency and the dissipation factor of the quartz resonant standing wave. In fact, figure 8(C) shows the frequency dependence of the real part of the admittance (conductance) of the nano-QCM when immersed in DI water (purple line) and in ethanol (green line); the peaks of the admittances clearly have both different shapes and centres. For comparison, figure 8(D) shows that, despite the zoom (for graphical clarity the *x*-axis is enlarged), the corresponding curves of a bare QCM in DI water (purple line)

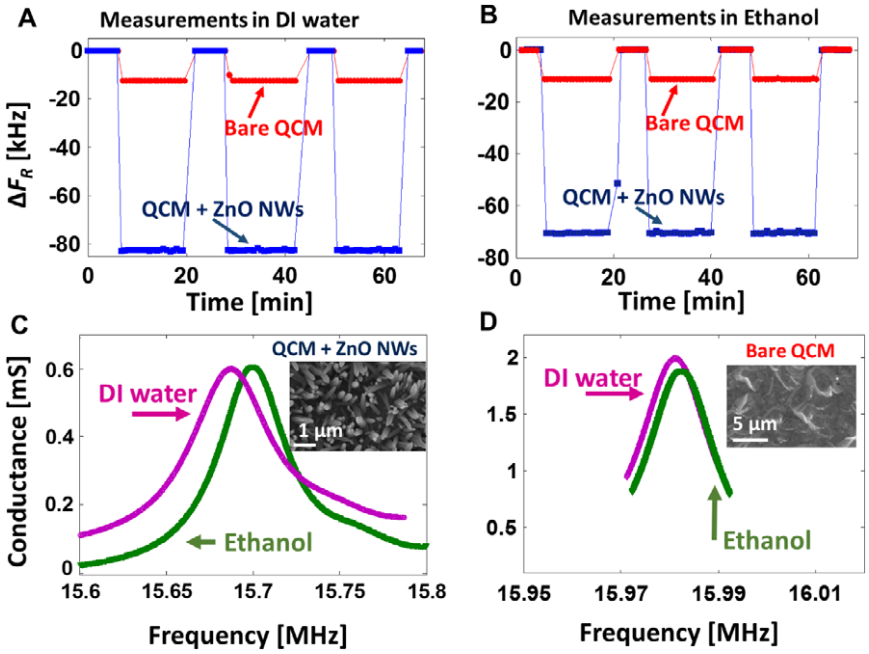

Figure 8. ΔF_R of a nano-QCM (blue line) and of a bare QCM (red line), with original resonant frequency of 16 MHz, upon immersion in DI water (A) and in ethanol (B) as measured by a network analyser. (C) Real part of the admittance of the nano-QCM during the immersion in DI water (purple line) and ethanol (green line). (D) Real part of the admittance of the bare QCM during the immersion in DI water (purple line) and ethanol (green line). The insets in (C) and (D) show SEM images of the nano-QCM (C) and the bare quartz (D).

Table 1. Frequency shift of a nano-QCM and a bare QCM upon immersion in water and ethanol.

		ΔF_R (air–ethanol)	ΔF_R (air–water)	ΔF_R (ethanol–water)
Original resonant frequency 16 MHz	Nano-QCM	70.330 kHz	82.343 kHz	12.013 kHz
	Bare QCM	11.163 kHz	12.438 kHz	1.275 kHz
	Ratio (R)	6.3	6.6	9.4
Original resonant frequency 20 MHz	Nano-QCM	142.501 kHz	159.069 kHz	16.568 kHz
	Bare QCM	13.594 kHz	15.001 kHz	1.407 kHz
	Ratio (R)	10.5	10.6	11.8

and in ethanol (green line) are hardly distinguishable (both resonant frequency and shape of the peak).

The theoretical shift of a perfectly smooth QCM immersed in a Newtonian liquid may be modelled by the Kanazawa equation [29]

$$\Delta F_R = -f_0^{1.5} C_q (\rho_l \eta_l / \pi)^{0.5}, \quad (5)$$

where ρ_l and η_l are the liquid density and viscosity, respectively. With the Kanazawa equation, the frequency shift for a 16 MHz QCM would be 7.97 kHz for ethanol and 8.182 kHz for DI water, with a 212 Hz difference between the two liquids. As is evident from figures 8(A) and (B), the measured shifts of the resonant frequencies of the bare QCMs are slightly higher, which may likely depend on dipole trapping at the solid–liquid interface [30] and on the un-polished surface of the silver electrode; however, the high-density, well-separated ZnO nanowires further increase the sensitivity by about one order of magnitude.

Table 1 quantitatively summarizes the resonant frequency shifts (ΔF_R) obtained upon immersion in water and ethanol for the four quartz sensors, namely the two bare QCMs (16 and 20 MHz) and the two nano-QCMs (16 and 20 MHz original resonant frequencies). As is evident, the ratio R between the resonant frequency shifts of the nano-QCM and the bare QCM is about 9.4 for the 16 MHz nano-QCM and about 11.8 for the 20 MHz nano-QCM.

Remarkably, the resonant frequency shifts of the nano-QCMs are the highest ever reported responses to liquid immersion for both water and ethanol. For instance, with reference to other techniques used for enhancing the sensitivity of QCMs to liquid properties, surface micropatterning [31–33] allowed sensitivities only slightly larger than those of our bare QCMs (whose high sensitivities are likely attributed to the high initial resonant frequencies and to the un-polished electrode surfaces). Similarly, nanostructuring of the QCM surface by using nanoporous alumina [34] and mesoporous titanium dioxide [35] only resulted in a maximum frequency shift water–ethanol of about 4 kHz [35], which is much less than with our devices (about 12 kHz for the 16 MHz nano-QCM and more than 16 kHz for the 20 MHz nano-QCM).

2. Conclusions

Here we have demonstrated that, by immersing standard, ultra-low-cost quartz resonators with silver electrodes in conventional zinc nitrate/HMTA equimolar nutrient solutions, without any seed layer or thermal annealing step, the gentle contamination from the metallic package promotes the high-density (up to 10 μm^{-1}) growth, on the electrodes, of well-separated, vertically aligned ZnO nanowires. The shape and density of the nanostructures can be tuned from nanotips to nanorods by changing the concentration of zinc nitrate and HMTA salts from 0.5 to 5 mM. By taking advantage of EDS, XRD, and PL measurements we have verified that the weak contamination from the metallic package only results in a low doping of the nanowires. Our results provide insight into the wet-chemistry synthesis of ZnO nanowires; besides, the combination of high-density and good separation is ideal for fabricating transducers with very large active areas, i.e. with very high sensitivities. The process is extremely simple and, unlike previous approaches, does not pose risks for the integrity of high-frequency quartz resonators that are typically very small and fragile and, therefore, difficult to handle. Moreover, the single-step fabrication process results in packaged devices which are ready to use. As an example of application, we have grown high-density arrays of well-separated ZnO nanowires on conventional, ultra-low-cost, packaged, and high-frequency (i.e. high sensitivity) quartzes and, as a preliminary test, we have demonstrated that the sensitivity to liquid properties of high-frequency (i.e. high sensitivity) quartzes can be further increased by nearly a factor of ten by the growth of nanowires. Our devices have obtained the highest ever reported shifts of the QCM resonant frequencies in response to immersion in both ethanol and water.

3. Methods

We prepared the nutrient solution for the synthesis of ZnO nanowires by mixing zinc nitrate and HMTA salts bought from Sigma Aldrich with ultrapure DI water obtained with a Barnstead Easypure II filtration system. We used a 1:1 proportional ratio of the two reagents with salt concentrations ranging from 0.5 to 5 mM. As deposition substrates, we used quartzes with silver electrodes bought from Fox Electronics (e.g. FOXLF200-20) and from Euroquartz (e.g. 20.000 MHz HC49/30/50/ − 40 + 85/18 pF/ATF). These quartzes come with a metallic HC-49/U package type (see figure 1(A)). The cap was opened by cutting the metallic cover near the base (e.g. by using a Dremel cutting tool) and, subsequently, the pins were inserted onto a custom-made Teflon bar located at the centre of a Pyrex bottle filled with 250 ml of the nutrient solution (total volume of about 325 ml) and kept in a vertical position; then, the system was immersed in a pre-heated water bath at 90 °C. Scanning electron microscope (SEM) images were taken with an FE-SEM (LEO SUPRA 1250, Oberkochen, Germany) after covering the samples with a thin gold layer. EDS was performed with a Quanta INCA system. $\theta/2\theta$ XRD scans were performed with a Rigaku diffractometer in Bragg–Brentano configuration equipped with Cu Kα radiation. Steady-state PL spectra were recorded with a standard laboratory set-up comprising a photomultiplier optical detector (Hamamatsu R3896) located at the output port of a 25 cm monochromator (Oriel Cornerstone 260-74 100); the excitation light beam was provided by the monochromatized output of a Hg(Xe) 200-W discharge lamp (Oriel 66485) at the wavelength $\lambda_{ex} =$ 290 nm; PL data were corrected for the spectral response of the apparatus that was calibrated with a reference black-body lamp. The QCM admittance spectra were recorded before and after the ZnO NW growth by an Agilent E5070 network analyser. For the measurements with QCMs immersed in ethanol (99.8% grade bought from Carlo Erba Reagenti Srl) and DI water, a special cap was prepared in order to immerse the two QCMs (bare QCM and nano-QCM) at the same time, with the electrodes a few millimetres within the liquid, and to contemporarily seal the container.

Acknowledgments

This work was financially supported by the Italian Institute of Technology Project Seed ‘API NANE’ and by the Italian Ministry for University and Research (FIRB—Futuro in Ricerca 2010 Project ‘Nanogeneratori di ossido di zinco ad altissima efficienza per l’alimentazione di microsistemi impiantabili e di reti wireless di sensori’). We also thank Professors Arnaldo D’Amico, Corrado Di Natale and Eugenio Martinelli and Drs Vito Errico and Giuseppe Arrabito for valuable discussions, and Massimo Palmacci, Ivan Pini and Stefano Petrocco for helping in the preparation of the experimental equipment.

References

[1] Lucklum R, Behling C and Hauptmann P 1999 Role of mass accumulation and viscoelastic film properties for the response of acoustic-wave-based chemical sensors *Anal. Chem.* **71** 2488–96

[2] Chen X, Wong C K Y, Yuan C A and Zhang G 2013 Nanowire-based gas sensors *Sensors Actuators* B **177** 178–95

[3] Patel N G, Huebner J S, Stadelmaier B E and Saredy J J 2010 *US Patent* US20100251802

[4] Pang L, Li J, Jiang J, Shen G and Yu R 2006 DNA point mutation detection based on DNA ligase reaction and nano-Au amplification: a piezoelectric approach *Anal. Biochem.* **358** 99–103

[5] Chu X, Zhao Z-L, Shen G-L and Yu R-Q 2006 Quartz crystal microbalance immunoassay with dendritic amplification using colloidal gold immunocomplex *Sensors Actuators* B **114** 696–704

[6] Huang H, Zhou J, Chen S, Zeng L and Huang Y 2004 A highly sensitive QCM sensor coated with Ag_+-ZSM-5 film for medical diagnosis *Sensors Actuators* B **101** 316–21

[7] Chao T W, Liu C J, Hsieh A H, Chang H M, Huang Y S and Tsai D S 2007 Quartz crystal microbalance sensor based on nanostructured IrO_2 *Sensors Actuators* B **122** 95–100

[8] Su P-G and Tsai J-F 2009 Low-humidity sensing properties of carbon nanotubes measured by a quartz crystal microbalance *Sensors Actuators* B **135** 506–11

[9] Jaruwongrungsee K, Wisitsoraat A, Tuantranont A and Lomas T 2008 *INEC 2008: 2nd IEEE Int. Nanoelectronics Conf.* pp 961–4
[10] Wang X, Zhang J and Zhu Z 2006 Ammonia sensing characteristics of ZnO nanowires studied by quartz crystal microbalance *Appl. Surf. Sci.* **252** 2404–11
[11] Zhang Y, Yu K, Ouyang S, Luo L, Hu H, Zhang Q and Zhu Z 2005 Detection of humidity based on quartz crystal microbalance coated with ZnO nanostructure films *Physica* B **368** 94–9
[12] Erol A, Okur S, Yağmurcukardeş N and Arıkan M Ç 2011 Humidity-sensing properties of a ZnO nanowire film as measured with a QCM *Sensors Actuators* B **152** 115–20
[13] Reyes P I *et al* 2009 A ZnO nanostructure-based quartz crystal microbalance device for biochemical sensing *IEEE Sensors J.* **9** 1302–7
[14] Ramakrishnan N, Nemade H B and Palathinkal R P 2011 Mass loading in coupled resonators consisting of SU-8 micropillars fabricated over SAW devices *IEEE Sensors J.* **11** 430–1
[15] Lu Y, Chen Y and Zhang Z 2011 *US Patent* US7989851
[16] Xu S and Wang Z L 2011 One-dimensional ZnO nanostructures: solution growth and functional properties *Nano Res.* **4** 1013–98
[17] Lee D, Yoo M, Seo H, Tak Y, Kim W-G, Yong K, Rhee S-W and Jeon S 2009 Enhanced mass sensitivity of ZnO nanorod-grown quartz crystal microbalances *Sensors Actuators* B **135** 444–8
[18] Quy N V, Minh V A, Luan N V, Hung V N and Hieu N V 2011 Gas sensing properties at room temperature of a quartz crystal microbalance coated with ZnO nanorods *Sensors Actuators* B **153** 188–93
[19] Minh V A, Tuan L A, Huy T Q, Hung V N and Quy N V 2013 Enhanced NH_3 gas sensing properties of a QCM sensor by increasing the length of vertically orientated ZnO nanorods *Appl. Surf. Sci.* **265** 458–64
[20] Hsu J W P, Tian Z R, Simmons N C, Matzke C M, Voigt J A and Liu J 2005 Directed spatial organization of zinc oxide nanorods *Nano Lett.* **5** 83–6
[21] Xu S, Lao C, Weintraub B and Wang Z L 2011 Density-controlled growth of aligned ZnO nanowire arrays by seedless chemical approach on smooth surfaces *J. Mater. Res.* **23** 2072–7
[22] Liu J, Huang X, Li Y, Ji X, Li Z, He X and Sun F 2007 Vertically aligned 1D ZnO nanostructures on bulk alloy substrates: direct solution synthesis, photoluminescence, and field emission *J. Phys. Chem.* C **111** 4990–7
[23] Wen X, Wu W, Ding Y and Wang Z L 2012 Seedless synthesis of patterned ZnO nanowire arrays on metal thin films (Au, Ag, Cu, Sn) and their application for flexible electromechanical sensing *J. Mater. Chem.* **22** 9469–76
[24] McPeak K M, Le T P, Britton N G, Nickolov Z S, Elabd Y A and Baxter J B 2011 Chemical bath deposition of ZnO nanowires at near-neutral pH conditions without hexamethylenetetramine (HMTA): understanding the role of HMTA in ZnO nanowire growth *Langmuir* **27** 3672–7
[25] Kokotov M, Biller A and Hodes G 2008 Reproducible chemical bath deposition of ZnO by a one-step method: the importance of contaminants in nucleation *Chem. Mater.* **20** 4542–4
[26] Djurišić A B *et al* 2007 Defect emissions in ZnO nanostructures *Nanotechnology* **18** 095702
[27] Tam K H, Cheung C K, Leung Y H, Djuris A B, Fung S, Kwok W M, Chan W K, Phillips D L, Ding L and Ge W K 2006 Defects in ZnO nanorods prepared by a hydrothermal method *J. Phys. Chem.* B **110** 20865–71
[28] Joo J, Chow B Y, Prakash M, Boyden E S and Jacobson J M 2011 Face-selective electrostatic control of hydrothermal zinc oxide nanowire synthesis *Nature Mater.* **10** 1–6
[29] Kanazawa K K and Gordon J G II 1985 Frequency of a quartz microbalance in contact with liquid *Anal. Chem.* **1771** 1770–1
[30] Yang M and Thompson M 1993 Multiple chemical information from the thickness shear mode acoustic wave sensor in the liquid phase *Anal. Chem.* **65** 1158–68
[31] Martin S J, Frye G C and Wessendorf K O 1994 Sensing liquid properties with thickness-shear mode resonators *Sensors Actuators* A **44** 209–18
[32] Zhang C, Schranz S and Hauptmann P 2000 Surface microstructures of TSM resonators and liquid properties measurement *Sensors Actuators* B **65** 296–8
[33] Itoh A and Ichihashi M 2011 Separate measurement of the density and viscosity of a liquid using a quartz crystal microbalance based on admittance analysis (QCM-A) *Meas. Sci. Technol.* **22** 015402
[34] Goubaidoulline I, Reuber J, Merz F and Johannsmann D 2005 Simultaneous determination of density and viscosity of liquids based on quartz-crystal resonators covered with nanoporous alumina *J. Appl. Phys.* **98** 014305
[35] Schön P, Michalek R and Walder L 1999 Liquid density response of a quartz crystal microbalance modified with mesoporous titanium dioxide *Anal. Chem.* **71** 3305–10